

# CMB footprints of high scale non-thermal leptogenesis

Anish Ghoshal,<sup>1,\*</sup> Dibyendu Nanda,<sup>2,†</sup> and Abhijit Kumar Saha<sup>3,‡</sup>

<sup>1</sup>*Institute of Theoretical Physics, Faculty of Physics,  
University of Warsaw, ul. Pasteura 5, 02-093 Warsaw, Poland*

<sup>2</sup>*School of Physics, Korea Institute for Advanced Study, Seoul 02455, Korea*

<sup>3</sup>*School of Physical Sciences, Indian Association for the Cultivation of Science,  
2A & 2B Raja S.C. Mullick Road, Kolkata 700032, India*

We study the imprints of high scale non-thermal leptogenesis on cosmic microwave background (CMB) from the measurements of inflationary spectral index ( $n_s$ ) and tensor-to-scalar ratio ( $r$ ), which otherwise is inaccessible to the conventional laboratory experiments. We argue that non-thermal production of baryon (lepton) asymmetry from subsequent decays of inflaton to heavy right handed neutrinos (RHN) is sensitive to the reheating dynamics in early Universe after the end of inflation. Such dependence provides detectable imprints on the  $n_s - r$  plane which is well constrained by the Planck experiment. We investigate two separate cases, (i) inflaton decays to radiation dominantly and (ii) inflaton decays to RHN dominantly which subsequently decays to the SM particles to reheat the Universe adequately. We obtain the corresponding estimates for  $n_s$  and  $r$  and find the latter case to be more predictive in view of recent Planck/BICEP data. We furnish the results considering  $\alpha$ -attractor inflationary models, however the prescription proposed here is quite generic and can be implemented to various kinds of single field inflationary models given the conditions for non-thermal leptogenesis is satisfied.

## I. Introduction

Observation of neutrino oscillations at various neutrino reactor experiments manifests that neutrinos are massive and have non-zero mixings [1–8]. On cosmological front, the BBN (Big bang nucleosynthesis), CMBR (Cosmic microwave background radiation) and LSS (Large scale structure) measurements favor neutrino mass to remain in the sub-eV range. The simplest mechanism to fit the neutrino oscillation data and explain the origin of the Standard Model (SM) neutrino masses is the type-I seesaw mechanism [9, 10] where the SM is extended with three right handed neutrinos (RHN), singlet under SM gauge symmetry. Remarkably, such minimal extension can also explain the cosmic matter-antimatter asymmetry which is dubbed as baryon asymmetry of the Universe (BAU). The RH neutrinos present in the type-I seesaw model [9, 10] with lepton number violating (LNV) Majorana mass are inherently unstable and decay to SM Higgs plus leptons. This out-of-equilibrium decay process at 1-loop picks up CP violation (CPV) via the complex Yukawa couplings, leading to asymmetric decay in to the leptons than in the anti-lepton counterpart [11–14]. Thus the three Sakharov conditions being fulfilled, we can have successful baryogenesis in early universe when afterwards the lepton asymmetry partially gets converted to the positive baryon asymmetry that we observe today [11–14].

The production of lepton asymmetry at early stages of the Universe can be thermal [11, 15] or non-thermal [16–

30] in nature. In case of thermal leptogenesis, the reheating temperature has to be larger than the RH neutrino mass scale ( $M_N < T_R$ ) such that non-zero initial abundance of the RH neutrino can be created efficiently from the thermal bath. In the non-thermal case, the condition  $M_N < T_R$  is not a necessity. The required initial abundance of RHN can be alternatively created non-thermally from a heavy scalar decay present in the early Universe. The scalar field can be identified with the inflaton which leads to an accelerated expansion at the beginning of the universe, in order to solve the horizon and the flatness problems. The same field could also be responsible for quantum generation of the primordial fluctuations seeding the large scale structure (LSS) of the Universe (see [31] for a review).

Despite the elegant explanation for the tiny SM neutrino masses and the generation of matter-antimatter asymmetry, the seesaw mechanism is excruciatingly difficult to test in laboratories, since in order to successfully drive leptogenesis, the right-handed neutrino mass scale has to be above  $\gtrsim 10^9$  GeV (see, *e.g.*, [32])<sup>1, 2</sup>. The indirect tests for high scale leptogenesis of course exist based on neutrino-less double beta decay and lepton flavor and CP violating decays of mesons [35], via CP violation in neutrino oscillation [36, 37], by the structure of the mixing matrix [38], or from theoretical constraints stemming from the demand of Higgs vacuum remaining meta-stable

<sup>1</sup> This bound can be evaded in case of resonant production of lepton asymmetry in presence of nearly degenerate RH neutrino species [33]

<sup>2</sup> With some fine tuning, it is also possible to lower the scale of the non-resonant thermal leptogenesis to as low as  $10^6$  GeV [34].

\* anish.ghoshal@fuw.edu.pl

† dnanda@kias.re.kr

‡ psaks2484@iacs.res.in

in the early universe [39, 40]. And more recently Gravitational Waves (GW) of primordial origins like that from cosmic strings [41], domain walls [42], nucleating and colliding vacuum bubbles [43, 44] or other topological defects [45] and primordial blackholes [46] have been proposed to constrain as well shed some light on high-scale leptogenesis scenarios. Under these circumstances, it is necessary, although highly challenging to find new and complementary tests of such heavy neutrino sectors and consequently the leptogenesis mechanism.

Motivated by this, in this paper, we envisage the scope of tracing the fingerprints of high scale non-thermal leptogenesis at CMB experiments. If the lepton asymmetry is produced via from the transfer of energy density from inflaton sector to lepton sector, then the amount of final lepton asymmetry yield is dependent on the reheating history of the Universe. On the other hand, for a given a model of inflation the predictions of inflationary observables namely the spectral indices and tensor to scalar ratio is also influenced by the post-inflationary [47] physics *e.g.* number of e-folds during reheating era as speculated in ref. [47] and subsequently studied in details in Refs. [48–50]. The aforementioned two observations suggest that the non-thermal leptogenesis at early Universe is expected to leave non-negligible imprints in the CMB predictions for inflationary observables which we pursue in this paper<sup>3</sup>.

We revisit the inflatary reheating epoch [54, 55] in  $\alpha$ -attractor models of inflation [56–61]. Interestingly, when we take into account the non-thermal production of lepton asymmetry from tree level inflaton decay, the reheating temperature of the Universe (or the inflaton-radiation coupling) cannot be arbitrary, rather guided by the observed amount of baryon asymmetry of the Universe. This in turn provides a distinct prediction and constraints on the  $n_s - r$  plane, which turns out to be stronger than the one provided by PLANCK/BICEP experiment [62]. In our analysis, we have assumed that the inflaton decays perturbatively. We have separately shed light on two possible cases: (i) inflaton decays dominantly to radiation and (ii) tree level interaction between inflaton and radiation is absent. In the latter case, the reheating of the Universe is realized solely from the decay of RHNs. We have followed a detailed numerical approach considering finite epoch of perturbative reheating era. We obtain unique correlations between the inflation sector parameters (namely coupling coefficients of inflaton-radiation and inflaton-RHNs) and predictions for  $(n_s, r)$  values in order to have right amount of baryon asymmetry in the Universe. The second case where inflaton decays to RHNs and subsequently the out of equilibrium decay of RHN instigates reheating era, turns out to be more predictive in view of recent Planck/BICEP

data [62].

## II. $\alpha$ -attractor inflation model

A general form of the  $\alpha$ -attractor inflaton potential (known as E model) is read as [60],

$$V(\phi) = \Lambda^4 \left( 1 - e^{-\sqrt{\frac{2}{3\alpha}} \frac{\phi}{M_P}} \right)^{2n}, \quad (1)$$

where  $M_P$  stands for the reduced Planck scale and  $\Lambda$  represents a mass scale that determines the energy scale of the inflation. A special case of Eq.(1) with  $\alpha = 1$  and  $n = 1$  mimics the standard Higgs-Starobinsky inflaton potential [63]. We first calculate the spectral index ( $n_s$ ) under the slow roll approximation to express it in terms of the model parameters  $\alpha$  and  $n$ .

$$n_s = 1 - \frac{8n \left( e^{\sqrt{\frac{2}{3\alpha}} \frac{\phi_k}{M_P}} + n \right)}{3\alpha \left( e^{\sqrt{\frac{2}{3\alpha}} \frac{\phi_k}{M_P}} - 1 \right)^2}, \quad (2)$$

where  $\phi_k$  is the inflaton field value at horizon exit. This can be simply translated to write  $\phi_k$  as function of  $n_s$ .

$$\phi_k = \sqrt{\frac{3\alpha}{2}} M_P \ln(1 + \Delta(n_s)), \quad (3)$$

where  $\Delta(n_s) = \frac{4n + \sqrt{16n^2 + 24\alpha n(1-n_s)(1+n)}}{3\alpha(1-n_s)}$ . Next, we make an estimate for the inflaton field value at the end of inflation by equating one of the slow roll parameters ( $\max[\epsilon, \eta]$ ) to unity as given by,

$$\phi_{\text{end}} = \sqrt{\frac{3\alpha}{2}} M_P \ln \left( \frac{2n}{\sqrt{3\alpha}} + 1 \right). \quad (4)$$

Utilizing Eq.(3) and Eq.(4), we compute quantities namely tensor to scalar ratio and the number of e-fold analytically which are given by,

$$\begin{aligned} r &= \frac{64n^2}{3\alpha \left( e^{\sqrt{\frac{2}{3\alpha}} \frac{\phi_k}{M_P}} - 1 \right)^2} \\ &= \frac{192\alpha n^2 (1 - n_s)^2}{\left[ 4n + \sqrt{16n^2 + 24\alpha n(1 - n_s)(1 + n)} \right]^2}, \end{aligned} \quad (5)$$

$$N_k = \frac{3\alpha}{4n} \left[ e^{\sqrt{\frac{2}{3\alpha}} \frac{\phi_k}{M_P}} - e^{\sqrt{\frac{2}{3\alpha}} \frac{\phi_{\text{end}}}{M_P}} - \sqrt{\frac{2}{3\alpha}} \frac{(\phi_k - \phi_{\text{end}})}{M_P} \right]. \quad (6)$$

The scalar potential at the end of inflation and the scalar perturbation spectrum are obtained as,

$$V_{\text{end}} = \Lambda^4 \left( \frac{2n}{2n + \sqrt{3\alpha}} \right)^{2n}, \quad (7)$$

$$A_s = \frac{3V(\phi_k)}{4\pi^2 r}. \quad (8)$$

<sup>3</sup> The impact of dark matter production at very early Universe on the inflationary observables have been studied by the authors of [51–53].

The observed value of  $A_s^{\text{obs}} = 2.2 \times 10^{-9}$  [64] precisely fixes one of the model parameters  $\Lambda$  as,

$$\Lambda = M_P \left( \frac{3\pi^2 r A_s^{\text{obs}}}{2} \right)^{1/4} \times \left[ \frac{2n(1+2n) + \sqrt{4n^2 + 6\alpha(1+n)(1-n_s)}}{4n(1+n)} \right]^{n/2}. \quad (9)$$

It is worth mentioning that each of the quantities ( $r, N_k, V_{\text{end}}$  and  $\Lambda$ ) have been expressed exclusively in terms of three model parameters ( $n, \alpha$  and  $n_s$ ). This will be immensely useful in connecting the lepton asymmetry from the RHN decay to the inflationary observables as we will describe in a while.

### III. Non-thermal Leptogenesis from inflaton decay

We envisage a picture where the inflaton  $\phi$  slowly dissipates its energy perturbatively by decays of individual inflaton quanta into lighter particles. This happens if the inflaton interactions (couplings) are sufficiently small such that the effective mass of inflaton decay-modes (which oscillates due to its coupling to  $\phi$ ) changes only adiabatically, and additionally if the occupation numbers in the primordial plasma at all times remain small to such an extent that the feedback of produced decay products on the  $\phi$ -field evolution is negligible. In this scenario,  $\Gamma_\phi$  is expected to remain constant during the reheating phase and only depends on the parameters as introduced in the Lagrangian  $\mathcal{L}_\phi$ . Assuming, the above mentioned arguments hold true, we have adopted the perturbative theory of reheating in the present set up.

To embed the non-thermal leptogenesis in the inflationary framework we propose the following Lagrangian in a model independent manner:

$$-\mathcal{L} \supset y_N \phi \bar{N}^C N + y_R \phi \bar{X} X + Y_\nu \bar{l}_L \tilde{H} N + M_N \bar{N}^C N + h.c., \quad (10)$$

where  $X$  represents a Dirac fermion which is part of the radiation bath after the completion of reheating era. The  $N$  (having bare mass  $M_N$ ) is the RH neutrino which decays to SM leptons ( $l_L$ ) and Higgs ( $H$ ) and subsequently contribute to the yield of lepton asymmetry. We assume all the coupling coefficients  $y_N, y_R$  real and positive. The neutrino Yukawa coupling  $Y_\nu$  could be complex and source the CP violation in the SM lepton sector. In the present analysis we deal with sufficiently small Yukawa couplings  $y_N$  and  $y_R$  such that they do not disturb the shape of the inflationary potential through radiative corrections. The first term in Eq.(10) leads to the non-thermal production of  $N$  from tree level inflaton decay. Whereas, the second term is responsible for inflaton decay to radiation at tree level. The third term triggers the out of equilibrium decay of RHN to SM leptons. In

principle it is preferred to add three singlet RH neutrinos or at least two in order to satisfy the neutrino oscillation data [65]) in the usual type-I seesaw framework. We consider here  $N_{2,3}$  being larger than the inflaton mass and hence their production from inflaton decay is expected to be suppressed. On the other hand,  $N_1$  is considered to be lighter than the inflaton and can be produced efficiently. In view of this, we ignore the dynamics of  $N_2$  and  $N_3$  and track the evolution of  $N_1$  only which is same as  $N$  in Eq.(10). As mentioned in the introduction section, we will examine two distinct cases: **(i)** inflaton dominantly decays to radiation and reheats the Universe *i.e.*  $\text{Br}_{\phi \rightarrow XX} > \text{Br}_{\phi \rightarrow NN}$  and **(ii)** inflaton decays to RHN first and its further decay to  $SU(2)_L$  doublets reheats the Universe which implies  $y_R \ll y_N$ . For simplicity, we have assumed that both the inflaton and RHN decay perturbatively. We define the decay widths of  $\phi$  to both radiation and  $N$  as given by [28],

$$\Gamma_\phi^N = \frac{|y_N|^2 m_\phi}{16\pi} \left( 1 - \frac{4M_N^2}{m_\phi^2} \right)^{3/2}, \quad \Gamma_\phi^R \simeq \frac{|y_R|^2 m_\phi}{8\pi}, \quad (11)$$

while the decay width for the RHN is  $\Gamma_N \simeq \frac{|Y_\nu|^2 M_N}{16\pi}$ . In the above, we have considered the SM particles being much lighter than the inflaton. The set of Boltzmann equations that govern the evolution of energy densities of various species, number densities for  $N$  and the yield of lepton asymmetry is given by [28]:

$$\frac{d\rho_\phi}{dt} + 3H(p_\phi + \rho_\phi) = -\Gamma_\phi^N \rho_\phi - \Gamma_\phi^R \rho_\phi, \quad (12)$$

$$\frac{d\rho_R}{dt} + 3H(p_R + \rho_R) = \Gamma_\phi^R \rho_\phi + \Gamma_N \rho_N, \quad (13)$$

$$\frac{d\rho_N}{dt} + 3H(p_N + \rho_N) = \Gamma_\phi^N \rho_\phi - \Gamma_N \rho_N, \quad (14)$$

$$\frac{dn_{B-L}}{dt} + 3Hn_{B-L} = -\frac{\varepsilon \rho_N \Gamma_N}{M_N}, \quad (15)$$

where  $\varepsilon$  is the CP asymmetry parameter. In the Boltzmann equation for  $n_{B-L}$ , we have ignored the washout effects since it is expected to be suppressed in case of non-thermal production of lepton asymmetry. The lepton asymmetry as obtained from Eq.(15) can be converted to the baryon asymmetry induced by the *sphaleron* process as given by [32],

$$\frac{n_B}{s} = -\left( \frac{8}{23} \right) \times \frac{n_{B-L}}{s}. \quad (16)$$

The experimentally observed value of  $\frac{n_B}{s}$  is  $8.7 \times 10^{-11}$  [64].

### IV. CMB imprints of non-thermal leptogenesis

The amount of lepton asymmetry yield from inflaton decay is proportional to the reheating temperature of the

Universe and the branching ratio of the the inflaton decay to RH neutrinos as depicted by the relation, [66, 67]:

$$\frac{n_{B-L}}{s} \approx \frac{3}{2} \times \text{Br}_{\phi \rightarrow \text{NN}} \times \left( \frac{\varepsilon T_R}{m_\phi} \right) \quad (17)$$

Note that, Eq.(17) holds under the instantaneous decay width approximation. Here in order to deliver an accurate description of particle production during reheating era, we follow the numerical approach, considering a finite reheating epoch. In fact, it is appraised earlier [68, 69] that the maximum temperature of the Universe ( $T_{\text{max}}$ ) turns out be always a few order larger than the original reheating temperature ( $T_{\text{RH}}$ ) of the Universe under the non-instantaneous perturbative reheating consideration. Therefore, a more relevant condition for the non-thermalisation of the RHN in the early Universe would be  $M_N < T_{\text{max}}$  instead of  $M_N < T_{\text{RH}}$ . This fact further enlightens the importance of solving the Boltzman equations Eqs. (12-15) for particle production considering a finite reheating epoch <sup>4</sup>.

Considering FRW ansatz, the e-folding number from the end of inflation to the end of reheating epoch is written as

$$N_{\text{re}} = \ln \left( \frac{a_{\text{re}}}{a_{\text{end}}} \right) = -\frac{1}{3(1 + \bar{\omega}_{\text{re}})} \ln \left( \frac{\rho_{\text{re}}}{\rho_{\text{end}}} \right), \quad (18)$$

where  $a_{\text{end}}$  and  $a_{\text{re}}$  are the corresponding scale factors at end of inflation and end of reheating respectively having respective energy densities,  $\rho_{\text{re}}$  and  $\rho_{\text{end}}$ . The quantity  $\rho_{\text{re}}$  can be computed numerically by solving the set of Boltzman equations (see Eqs. (12-15)). In Eq.(18), the averaged equation state from the end of inflation to end of reheating is indicated by  $\bar{\omega}_{\text{re}}$  which is defined as,

$$\bar{\omega}_{\text{re}} = \frac{1}{N_{\text{re}}} \int_0^{N_{\text{re}}} \omega(N_e) dN_e. \quad (19)$$

It is shown in [72], that the equation of state parameter during oscillation era is approximately  $\bar{\omega}_{\text{re}} \approx \frac{n-1}{n+1}$  for a generic inflationary potential  $V(\phi) \propto \phi^n$  <sup>5</sup>. Now at horizon exit  $k = a_k H_k$ , and one can write

$$\ln \left( \frac{k}{a_k H_k} \right) = \ln \left( \frac{a_{\text{end}}}{a_k} \frac{a_{\text{re}}}{a_{\text{end}}} \frac{a_0}{a_{\text{re}}} \frac{k}{a_0 H_k} \right) = 0, \quad (20)$$

where  $a_0$  stands for the scale factor at present time. This further implies,

$$N_k + N_{\text{re}} + \ln \left( \frac{a_0}{a_{\text{re}}} \right) + \ln \left( \frac{k}{a_0 H_k} \right) = 0. \quad (21)$$

Next task is to express the ratio  $\frac{a_{\text{re}}}{a_0}$  as function of  $N_{\text{re}}$ . Using entropy conservation principle in between the end of reheating and the present epoch, we find,

$$\frac{a_{\text{re}}}{a_0} = \left( \frac{43}{11g_{*s}} \right)^{1/3} \left( \frac{\pi^2 g_* T_0^4}{30\rho_{\text{re}}} \right)^{1/4}, \quad (22)$$

Further simplification of Eq.(22) is possible by connecting  $\rho_{\text{re}}$  to  $\rho_{\text{end}}$  (or  $V_{\text{end}}$ ) by Eq.(18). Now during inflation,

$$\rho = \frac{1}{2} \dot{\phi}^2 + V(\phi). \quad (23)$$

According to Klein Gordan equation (during inflation),

$$\ddot{\phi} + 3H\dot{\phi} + V'(\phi) = 0. \quad (24)$$

Assuming  $\ddot{\phi} \ll 3H\dot{\phi}$ ,  $V'(\phi)$  and  $H^2 \simeq \frac{V(\phi)}{3M_P^2}$ , we find from Eq.(23),

$$\rho \simeq V(\phi) \left( 1 + \frac{\epsilon}{3} \right). \quad (25)$$

Hence

$$\rho_{\text{end}} \simeq \frac{4}{3} V_{\text{end}}. \quad (26)$$

with  $\epsilon \sim 1$  near the end of inflation. We find the simplified relation between  $\rho_{\text{re}}$  and  $\rho_{\text{end}}$  as can be written as (following Eq.(18))

$$\rho_{\text{re}} = \frac{4}{3} V_{\text{end}} e^{-3N_{\text{re}}(1 + \bar{\omega}_{\text{re}})} \quad (27)$$

With this Eq.(22) can be translated into,

$$\ln \left( \frac{a_{\text{re}}}{a_0} \right) = \frac{1}{3} \ln \left( \frac{43}{11g_{*s}} \right) + \frac{1}{4} \left( \frac{\pi^2 g_*}{30} \right) + \frac{1}{4} \ln \left( \frac{3T_0^4}{4V_{\text{end}}} \right) + \frac{3N_{\text{re}}(1 + \bar{\omega}_{\text{re}})}{4}. \quad (28)$$

We replace Eq.(28) in Eq.(21) and use  $H_k = \frac{\pi M_P \sqrt{r A_s}}{\sqrt{2}}$  to obtain,

$$N_{\text{re}} = \frac{4}{3\omega_{\text{re}} - 1} \left[ N_k + \ln \left( \frac{k}{a_0 T_0} \right) + \frac{1}{4} \ln \left( \frac{40}{\pi^2 g_*} \right) + \frac{1}{3} \ln \left( \frac{11g_{*s}}{43} \right) - \frac{1}{2} \ln \left( \frac{\pi^2 M_P^2 r A_s}{2V_{\text{end}}^{1/2}} \right) \right]. \quad (29)$$

The RHS of Eq.(29) is purely a function of  $n_s$  once we fix  $\alpha, n$  and  $A_s = A_s^{\text{obs}}$  and replace  $r, N_k, V_{\text{end}}$  accordingly following Eqs.(5), (6) and (7) respectively. On the other hand, the LHS of Eq.(29), carrying the information of duration of reheating epoch. is a function of the radiation energy density after the completion of the reheating and can be obtained by solving Eqs. (12-15). hus, Eq.(29) manifests the clear dependence of  $n_s$  (and

<sup>4</sup> Once the RH neutrinos abundance is formed the inflaton later on can also mediate leptogenesis via higher-dimensional operators involved [70, 71]

<sup>5</sup> In  $\alpha$ -attractor models of inflation, the inflation potential mimics the form  $V(\phi) \propto \phi^n$  during reheating epoch.

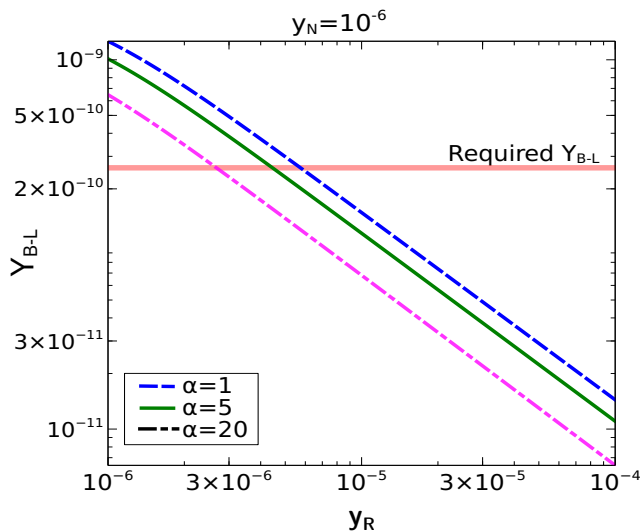


FIG. 1. The  $B-L$  yield is plotted in terms of  $y_2$  for different values of  $\alpha$  and for fixed  $y_1$ . The red band represents the observed value of  $Y_{B-L} = \frac{n_{B-L}}{s}$ .

$r$ ) on the  $N_{\text{re}}$  which is solely determined by the time required for the complete transfer of inflaton energy density to the radiation bath during reheating. Interestingly, in case of non-thermal leptogenesis, the RHN neutrino production and subsequently the baryon asymmetry of the Universe also rely on the reheating dynamics as evident from the coupled Boltzman equations in Eqs. (12-15)). These two observations open up the scope of understanding the dependence of lepton (baryon) asymmetry of the Universe on the inflationary observables  $n_s$  (and  $r$ ) on one hand and to probe the scale of leptogenesis on the other. The present study is aimed to examine such an intriguing connection quantitatively. To be specific, we attempt to find out whether requirement of producing the observed amount of baryon asymmetry can put further constraints in the  $(n_s, r)$  plane as already restricted by the Planck/BICEP data [62]. Throughout our analysis, we have used lepton asymmetry parameter  $\varepsilon = 10^{-6}$ , mass scale of the RH neutrino  $M_N = 10^{13}$  GeV and decay width of the RHN  $\Gamma_N = 10^{-11} M_P$ . These values are easily obtainable by utilizing the Casas Ibarra parametrisation [73] satisfying the neutrino oscillation data (see appendix A). We have also considered  $n = 1$  in the inflationary potential as it gives rise to a bare mass term for the inflaton field (during reheating) which is  $m_{\text{inf}}^2 = \frac{4\Lambda^4}{3\alpha M_P}$ .

## V. Results

We focus on two distinct cases separated by the interaction between inflaton with radiation and RHNs. In the first one, the reheating dominantly takes place from the tree level inflaton decay while in the second case, inflaton decays to RHN first and out of equilibrium decay of RHN

reheats the Universe. We discuss the results of these two cases separately below:

**Case I:** In this category, we have two independent parameters, namely  $y_N$  and  $y_R$  provided other relevant parameters (including  $\alpha$ ) are fixed as specified earlier. First in Fig. 1, we examine the dependence of comoving lepton asymmetry abundance  $Y_{B-L}$  ( $= \frac{n_{B-L}}{s}$ ) on the inflaton to radiation coupling coefficient  $y_R$  for various choices of  $\alpha$ . For the purpose we have fixed  $y_N = 10^{-6}$ . We observe that for a constant  $\alpha$ , the  $Y_{B-L}$  decreases with the increase of  $y_2$ . This can be understood in the following manner. In general, a larger  $y_R$  implies larger reheating temperature, however at the same time this leads to smaller branching ratio of the inflaton decaying into RHNs  $\text{Br}_{\phi \rightarrow NN}$ . In case of non-thermal leptogenesis  $Y_{B-L} \propto \text{Br}_{\phi \rightarrow NN} \times T_{\text{RH}}$  as per Eq.(17). Considering instantaneous reheating mechanism this translates to  $\propto \frac{1}{y_R}$  for a fixed  $y_N$ . This causes  $Y_{B-L}$  to decrease with  $y_R$  as observed in Fig. 1. We also highlight the correct range of  $Y_{B-L}$  (in lighter red) which can be converted to the observed baryogenesis in the Universe via sphaleron transition. This fixes the allowed value of  $y_R$  e.g.  $y_R \sim 5.8 \times 10^{-6}$  for  $\alpha = 1$ . It is also noticed that upon increasing  $\alpha$ , we require a smaller  $y_R$  to satisfy the baryon asymmetry bound. This attributes to the fact that a larger  $\alpha$  reduces the mass of the inflaton and in turn decreases the branching ratio  $\text{Br}_{\phi \rightarrow NN}$  which tends to suppress the final baryon asymmetry. Hence we need a smaller  $y_R$  in order to obtain correct amount of  $Y_{B-L}$  following the argument  $Y_{B-L} \propto \frac{1}{y_R}$  as earlier explained.

We show the evolutions of energy densities of inflaton, radiation and RH neutrino as function of scale factor in left panel of Fig. 2 considering a particular benchmark point (with  $\alpha = 5, y_N = 5 \times 10^{-7}$  and  $y_R = 10^{-6}$  and other parameters as fixed as earlier specified) that is able to address correct baryon asymmetry of the Universe. It is found that the energy density of  $N$  always remains below the  $\rho_R$  since in this case, the inflaton predominantly decays to radiation. Initially the Universe was  $\phi$  dominated and the crossover from  $\phi$  to radiation domination is marked by the ‘ $\star$ ’ symbol. In right panel of Fig. 2, the evolution of the temperature of the Universe is presented as function of the scale factor. We also find that the  $T_{\text{max}}$  turns out to be few order larger than the reheating temperature  $T_{\text{RH}}$  of the Universe as marked by the symbols ‘ $\bullet$ ’ and ‘ $\star$ ’ respectively. We also confirm that the condition for non-thermalisation is easily satisfied since  $T_{\text{max}}$  remains much below than the RH neutrino mass scale (as indicated by the red dashed line).

Next in Fig. 3 we provide contours of experimentally favored value of  $Y_{B-L} = 2.5 \times 10^{-10}$  in the  $y_R - y_N$  plane for three different values of  $\alpha = (1, 5, 20)$ . This figure shows that the required value of  $y_N$  increases with the enhancement of  $y_R$  to obtain experimentally favored  $Y_{B-L} = 2.5 \times 10^{-10}$  or *vice versa*. As earlier argued,  $Y_{B-L} \propto \frac{y_N^2}{y_R}$  and hence a larger value of  $y_R$  requires

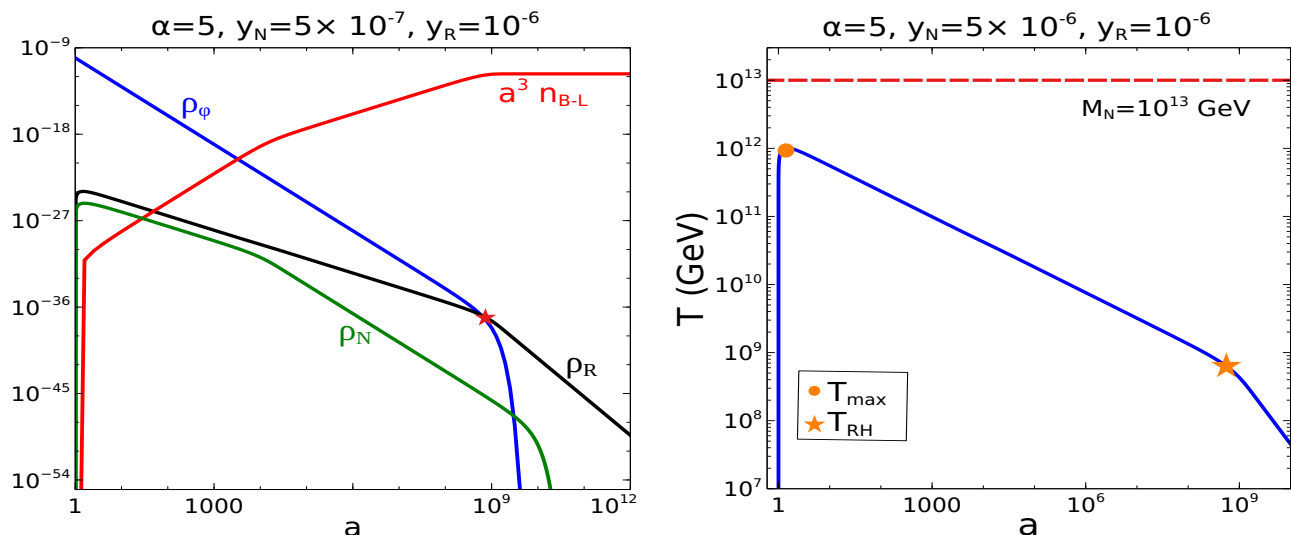


FIG. 2. [Left:] Evolutions for different energy densities of different components of the Universe as function of a scale factor. [Right] The temperature of the Universe is shown as a function of the scale factor. The red dashed line indicates the RH neutrino mass scale.

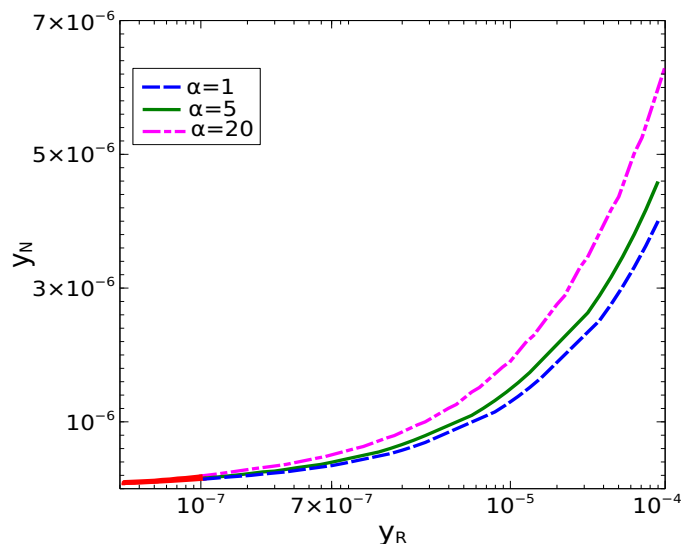


FIG. 3. Contours for  $Y_{B-L} = 2.5 \times 10^{-10}$  in  $y_R$ - $y_N$  plane for different values of  $\alpha$ . The red part of each contours distinguish the region where inflaton predominantly decays to RHN.

larger  $y_N$  to attain a particular  $Y_{B-L}$ . We also observe that a higher value of  $\alpha$  needs larger  $y_N$  for a fixed  $y_R$ . The reason for this particular pattern is explained earlier. We reiterate it here once again. The tree level inflaton mass is inversely proportional to  $\alpha$  and hence a larger  $\alpha$  means lighter inflaton which corresponds to reduced  $\text{Br}_{\phi \rightarrow NN}$  for a particular set of  $(y_N, y_R)$ . Thus one need to further tune  $y_N$  to a larger value to obtain the same  $Y_{B-L}$  as specified earlier. We also point out the region (in red) in each of  $Y_{B-L}$  contours where  $\text{Br}_{\phi \rightarrow NN} > \text{Br}_{\phi \rightarrow RR}$  where inflaton decays dominantly to the RHN. We keep  $y_R$  below  $\mathcal{O}(10^{-4})$  such that non-

perturbative effects during reheating do not turn important. Also this makes sure the inflationary potential do not receive large radiative corrections arising due to the the presence of neutrinos. We infer two important features from Fig. 3. Firstly, the values of  $y_R$  and  $y_N$  are correlated by the requirement of attaining correct order of baryon asymmetry. Secondly, we find that the shape of the inflaton potential (represented by varying  $\alpha$ ) leave some consequences on the estimate of numerical values for  $(y_N, y_R)$  to accommodate correct order of  $Y_{B-L}$ . We will see in a while that these combined effects leave non-negligible impact on the prediction of spectral index and tensor to scalar ratio of the  $\alpha$ -attractor inflation model.

In Fig. 4, we depict the observational consequence of successfully producing the right order of baryon asymmetry in the measurements of the inflationary observables namely  $n_s$  and  $r$ . In left panel, we utilize the allowed ranges for  $y_R$  from Fig. 3 for different  $\alpha$  in order to satisfy the baryon asymmetry of the Universe and find the predictions for spectral index  $n_s$ . Remember for each  $\alpha$ , a particular  $y_R$  corresponds to a definite value of  $y_N$  in Fig. 3. Increasing  $y_R$  leads to smaller  $N_{\text{re}} (> 0)$  according to Eq.(18) which translates into bigger  $n_s$ . With these observations, we can predict a distinct range for  $n_s$  for each  $\alpha$ . For example, with  $\alpha = 1$ , we find  $0.9616 \lesssim n_s \lesssim 0.9630$  while for  $\alpha = 20$ , the predicted range is  $0.9648 \lesssim n_s \lesssim 0.9664$ . In the right panel of Fig. 4, we use the  $n_s - r$  plane to show our findings, considering different values of  $\alpha$ . We also present the Planck/BICEP allowed  $1\sigma$  and  $2\sigma$  contours [62] in the same plane for comparison purpose. Here also we set the values of  $y_R$  and  $y_N$  as per Fig. 3 to obtain the estimate of  $(n_s, r)$ . It is noticed that for a constant value of  $\alpha$ , the predicted range of tensor to scalar ratio ( $r$ ) is strictly restricted. As an example, for  $\alpha = 1$ , we obtain

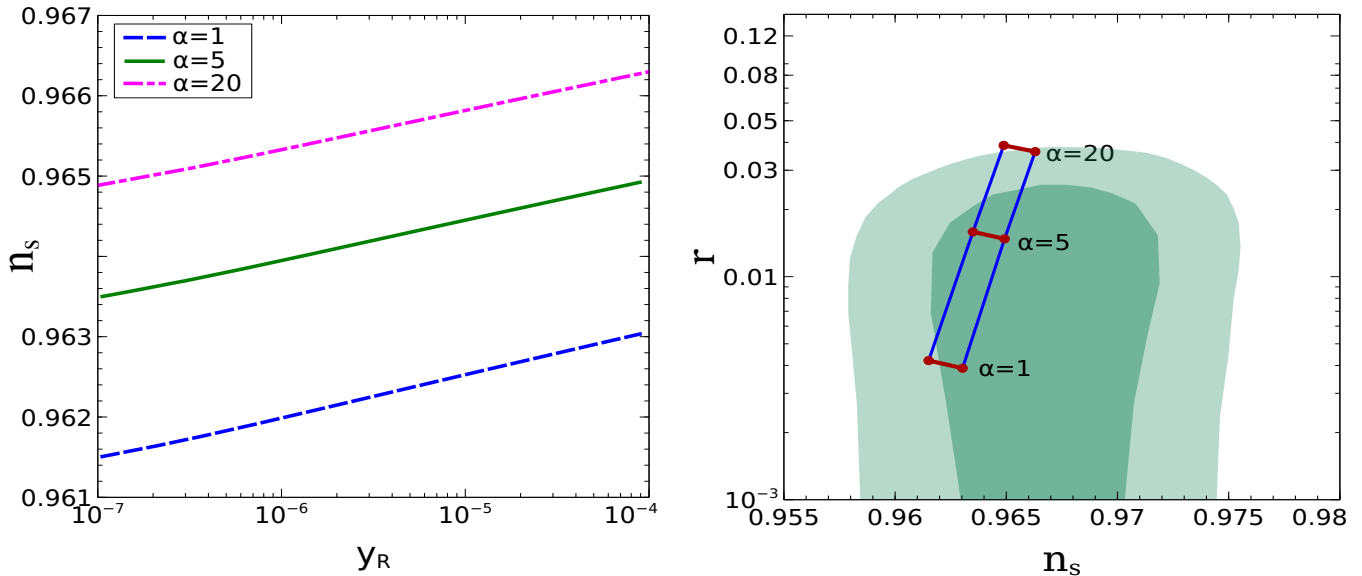


FIG. 4. [Left:] Allowed ranges of  $n_s$  in terms of  $y_R$  considering different values of  $\alpha$ . We fix the range of  $y_R$  according to Fig. 3 that yield the observed amount of baryon asymmetry in the Universe for suitable choices of  $y_N$ . [Right:] We show our predictions in the  $n_s - r$  plane against the Planck/BICEP  $1\sigma$  and  $2\sigma$  allowed region [62].

$0.0038 \lesssim r \lesssim 0.0044$  with  $0.9616 \lesssim n_s \lesssim 0.9630$  which provides us the correct value of baryon asymmetry in the Universe. Clearly, the requirement of successful baryogenesis indeed restricts the  $n_s - r$  plane which is stringent than the present Planck/BICEP data [62]. Note that the predicted region of  $(n_s - r)$  almost remains inside the sensitivity curves of Planck/BICEP data [62] (except a small portion of the  $\alpha = 20$  line). Therefore the recent Planck/BICEP data does not or very weakly constrain the the coupling parameters  $y_N$  and  $y_R$ . However future CMB experiments such as CBM-S4, STPOL, LITBIrd with improved sensitivities or more precise measurements of  $(n_s, r)$  could validate/refute our results.

**Case II:** The Case II effectively contains a single independent parameter which is  $y_N$  apart from  $\alpha$  since we have considered here  $y_R \simeq 0$ . The inflaton decays to RHN first and its subsequent out of equilibrium decay efficiently reheats the Universe. Therefore, in this case the reheating of the Universe is a two step process. Once  $\alpha$  is fixed, both the reheating and the production of baryon asymmetry will be controlled by  $y_N$  only. Once again, we have solved the set of Boltzmann equations (Eqns.(12 - 15)) numerically considering  $\Gamma_\phi^R \simeq 0$ . Then we obtain the value of  $n_s$  by solving Eq.(29) and subsequently  $r$  from Eq.(5). We present our results in Figs 5-6. We show the estimate of  $Y_{B-L}$  in terms of  $y_N$  for different values of  $\alpha$  in Fig 5. Increasing  $y_N$ , enhances the rate of RHN production as well as the reheating temperature which result into larger  $Y_{B-L}$ . On the other hand a larger  $\alpha$  reduces the inflaton mass which in turn suppresses the RHN production rate. To compensate that,

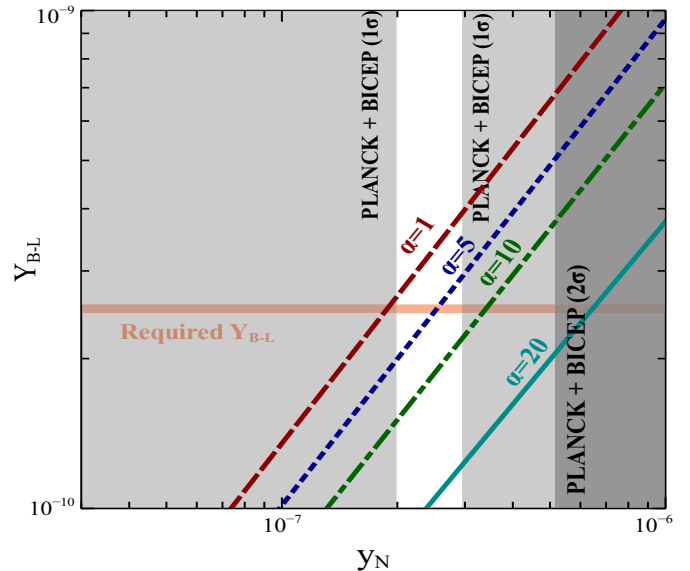


FIG. 5. Case II: The  $B - L$  yield is plotted in terms of  $y_N$  considering different values of  $\alpha$ . The shaded regions regions are obtained using the Planck+BICEP  $1\sigma$  and  $2\sigma$  bounds [62].

a larger  $y_N$  is required for larger  $\alpha$ . In Fig. 6, we show the  $n_s - r$  predictions for the case II. Next, we use the estimate of  $y_N$  from Fig 5 for a particular  $\alpha$  to compute  $r$ . We find here one to one correlation between  $y_N$  (that regulates both reheating as well as the baryons asymmetry of the Universe) and estimate of  $(n_s, r)$ . For example,  $\alpha = 5$  requires  $y_N \simeq 2.3 \times 10^{-7}$  which implies  $(n_s = 0.9632, r = 0.016)$ . It also turns out that simul-

taneous requirement of yielding sufficient baryon asymmetry and satisfying the Planck/BICEP ( $1\sigma$  and  $2\sigma$ ) data [62] poses strong bound on the amount of  $y_N$  as observed from Fig. 5 (shaded regions) and Fig. 6. The Planck/BICEP  $2\sigma$  data [62] restricts  $y_N$  to remain below  $\sim 5 \times 10^{-7}$  while the  $1\sigma$  data from same experiment imposes  $2 \times 10^{-6} \lesssim y_N \lesssim 3 \times 10^{-6}$ . We have performed a similar exercise considering  $M_N = 1.25 \times 10^{10}$  GeV and show the corresponding results for  $(n_s, r)$  in Fig. 6. Future measurements by CMB-S4, SPTpol, LitBIRD and CMB-Bharat with upgraded sensitivities will be able to further constraint or rule out the allowed range for  $y_N$  in view of Planck/BICEP data [62].

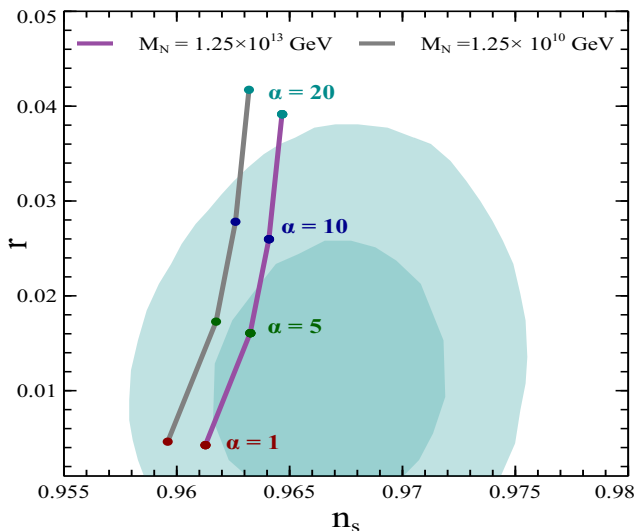


FIG. 6. *Case II: With the values of  $y_N$  obtained from Fig. 5 for different  $\alpha$  that give rise to observe baryon asymmetry, we find the corresponding predictions for  $n_s$  and  $r$  by fixing  $M_N$  at  $1.25 \times 10^{13}$  GeV (in purple). Following a similar procedure we also show the results for a somewhat lower  $M_N \sim 1.25 \times 10^{10}$  GeV (solid brown line). We also present the  $1\sigma$  and  $2\sigma$  allowed regions by Planck/BICEP [62] on the same plane.*

## VI. Conclusion

We re-analyse non-thermal production of matter-antimatter asymmetry in early universe via leptogenesis and investigated its impact on CMB predictions for inflationary observables namely spectral index and tensor to scalar ratio. Considering very massive RHN ( $\sim 10^{13}$  GeV), we reinforce that the final amount of lepton asymmetry yield crucially depends on the reheating dynamics of the Universe. Consequently we find that such correlations results into very predictive inflationary observable values  $(n_s, r)$ . Although for concrete predictions we considered the  $\alpha$ -attractor inflationary model for our exercise, the prescription presented here is generic and can be implemented to any inflationary scenario. We scrutinized two possible cases: (i) inflaton decays dominantly

to radiation and (ii) inflaton does not couple to radiation directly but a standard radiation dominated Universe is secured via inflaton decaying to heavy neutrinos and subsequently to radiation. In the first case we have two free parameters which are coefficients for inflaton to radiation coupling and inflaton to RHN coupling respectively when other relevant parameters like RHN mass scale, its decay width and  $\alpha$  are fixed. Using the requirement of producing sufficient baryon asymmetry, we have constrained the  $n_s$ - $r$  plane and find that the corresponding bound as obtained, appears stronger than the recent Planck-BICEP data [62]. For example, in Case I our analysis reveals that for  $\alpha = 5$ , successful baryogenesis via leptogenesis predicts  $0.9616 \lesssim n_s \lesssim 0.9630$  with  $0.0038 \gtrsim r \gtrsim 0.00437$ . In the latter case, we have a single independent parameter which is inflaton to RHN coupling coefficient. We obtain unique correlations between  $y_N$  and  $(n_s - r)$  values for a constant  $\alpha$  that leads to successful baryogenesis in the early Universe. For example,  $\alpha = 5$  requires  $y_N \simeq 2.3 \times 10^{-7}$  to yield correct order of baryon asymmetry which implies  $n_s = 0.9632$  and  $r = 0.015$ . Interestingly in the second case, the Planck+BICEP  $1\sigma$  and  $2\sigma$  data [62] for  $(n_s, r)$  severely restricts the amount of  $y_N$ . In particular the  $1\sigma$  bound on  $(n_s, r)$  by Planck+BICEP [62] imposes  $y_N$  to remain inside a very narrow region. Fig. 6 further depicts that a somewhat lower value of RHN mass scale ( $\sim 10^{10}$  GeV) is already ruled out by the Planck+BICEP  $1\sigma$  data [62]. Future CMB experiments with improved sensitivities like LitBIRD, SPT-pol, CMB-S4, CMB-HD, CMB-Bharat and others [74–86]) will be able to eliminate part of the parameter space further that gives rise to consistent non-thermal leptogenesis (baryogenesis) scenario. In summary, the present study provides a scope to indirectly test a high scale non-thermal leptogenesis which is out of reach of conventional neutrino experiments, colliders or astrophysical observations. The prescription is general as  $\alpha$ -attractor encapsulates generic large-field inflationary scenarios and can be applied to any kind of inflationary models. Particularly, it would be intriguing to analyse the impact of high scale non-thermal leptogenesis (baryogenesis) on the small field inflationary models which we plan to pursue in future and is beyond the scope of the current analysis.

## VII. Acknowledgements

DN would like to thank Arghyajit Datta for various discussions. AG thanks Anupam Mazumdar and Marco Drewes for discussions. AKS is supported by NPDR grant PDF/2020/000797 from Science and Engineering Research Board, Government of India. The work of DN is supported by National Research Foundation of Korea (NRF)'s grants, grants no. 2019R1A2C3005009(DN).



### A. Casas-Ibara parameterization

In a general type-I seesaw framework, we note the presence of heavy three RH neutrinos in order to satisfy neutrino oscillation data by making the three SM neutrinos massive. The CP asymmetry produced from the decay of lightest right handed neutrinos can be written as [14],

$$\varepsilon = \frac{1}{8\pi} \sum_{j \neq 1} \frac{\text{Im} \left[ (y_\nu^\dagger y_\nu)_{1j}^2 \right]}{(y_\nu^\dagger y_\nu)_{11}} \mathcal{F} \left( \frac{M_j^2}{M_1^2} \right) \quad (\text{A1})$$

where  $\mathcal{F} \approx 3/4\sqrt{x}$ . Adopting the familiar Casas-Ibara parameterization the Yukawa matrix  $y_\nu$  can be written as [73]

$$y_\nu = \frac{\sqrt{2}}{v} U_{\text{PMNS}} \sqrt{m_\nu^d} \mathcal{R}^T \sqrt{M_N} \quad (\text{A2})$$

where  $\mathcal{R}$  is  $3 \times 3$  orthogonal matrix and is chosen as [87],

$$\mathcal{R} = \begin{pmatrix} \cos \theta & \sin \theta & 0 \\ -\sin \theta & \cos \theta & 0 \\ 0 & 0 & 1 \end{pmatrix} \quad (\text{A3})$$

In this representations the free parameters are the masses of the RHNs and the rotational angle  $\theta$  of the matrix  $\mathcal{R}$ . We have chosen the following set of benchmark values,

$$M_{N_1} = 10^{13} \text{ GeV}, M_{N_2} = 5 \times 10^{13} \text{ GeV}, M_{N_3} = 10^{14} \text{ GeV}$$

and,  $\theta = 0.16 + 0.5i$ . We find the neutrino Yukawa matrix as,

$$y_\nu = \begin{pmatrix} 0.0588 - 0.0152i & 0.0584 + 0.0483i & -0.0605i \\ -0.0214 - 0.0289i & 0.0940 - 0.0221i & 0.2675 \\ 0.0156 + 0.0136i & -0.0722 + 0.0077i & 0.3080 \end{pmatrix} \quad (\text{A4})$$

which yields  $\varepsilon_1 \sim 10^{-6}$  and  $\Gamma_{N_1} \sim 10^{-11} M_P$ .

- 
- [1] S. Fukuda et al. (Super-Kamiokande), *Phys. Rev. Lett.* **86**, 5656 (2001), arXiv:hep-ex/0103033.
- [2] S. Fukuda et al. (Super-Kamiokande), *Phys. Lett. B* **539**, 179 (2002), arXiv:hep-ex/0205075.
- [3] Y. Ashie et al. (Super-Kamiokande), *Phys. Rev. D* **71**, 112005 (2005), arXiv:hep-ex/0501064.
- [4] Q. R. Ahmad et al. (SNO), *Phys. Rev. Lett.* **89**, 011301 (2002), arXiv:nucl-ex/0204008.
- [5] S. Abe et al. (KamLAND), *Phys. Rev. Lett.* **100**, 221803 (2008), arXiv:0801.4589 [hep-ex].
- [6] K. Abe et al. (T2K), *Phys. Rev. Lett.* **107**, 041801 (2011), arXiv:1106.2822 [hep-ex].
- [7] Y. Abe et al. (Double Chooz), *Phys. Rev. Lett.* **108**, 131801 (2012), arXiv:1112.6353 [hep-ex].
- [8] K. Abe et al. (T2K), *Phys. Rev. Lett.* **112**, 061802 (2014), arXiv:1311.4750 [hep-ex].
- [9] R. N. Mohapatra and G. Senjanovic, *Phys. Rev. Lett.* **44**, 912 (1980).
- [10] P. Minkowski, *Phys. Lett. B* **67**, 421 (1977).
- [11] M. Fukugita and T. Yanagida, *Phys. Lett. B* **174**, 45 (1986).
- [12] M. A. Luty, *Phys. Rev. D* **45**, 455 (1992).
- [13] M. Plumacher, *Z. Phys. C* **74**, 549 (1997), arXiv:hep-ph/9604229.
- [14] L. Covi, E. Roulet, and F. Vissani, *Phys. Lett. B* **384**, 169 (1996), arXiv:hep-ph/9605319.
- [15] G. F. Giudice, A. Notari, M. Raidal, A. Riotto, and A. Strumia, *Nucl. Phys. B* **685**, 89 (2004), arXiv:hep-ph/0310123.
- [16] G. Lazarides and Q. Shafi, *Phys. Lett. B* **258**, 305 (1991).
- [17] H. Murayama, H. Suzuki, T. Yanagida, and J. Yokoyama, *Phys. Rev. Lett.* **70**, 1912 (1993).
- [18] E. W. Kolb, A. D. Linde, and A. Riotto, *Phys. Rev. Lett.* **77**, 4290 (1996), arXiv:hep-ph/9606260.
- [19] G. F. Giudice, M. Peloso, A. Riotto, and I. Tkachev, *JHEP* **08**, 014 (1999), arXiv:hep-ph/9905242.
- [20] T. Asaka, K. Hamaguchi, M. Kawasaki, and T. Yanagida, *Phys. Lett. B* **464**, 12 (1999), arXiv:hep-ph/9906366.
- [21] T. Asaka, K. Hamaguchi, M. Kawasaki, and T. Yanagida, *Phys. Rev. D* **61**, 083512 (2000), arXiv:hep-ph/9907559.
- [22] R. Jeannerot, S. Khalil, and G. Lazarides, *Phys. Lett. B* **506**, 344 (2001), arXiv:hep-ph/0103229.
- [23] K. Hamaguchi, H. Murayama, and T. Yanagida, *Phys. Rev. D* **65**, 043512 (2002), arXiv:hep-ph/0109030.
- [24] T. Asaka, H. B. Nielsen, and Y. Takanishi, *Nucl. Phys. B* **647**, 252 (2002), arXiv:hep-ph/0207023.
- [25] V. N. Senoguz, *Phys. Rev. D* **76**, 013005 (2007), arXiv:0704.3048 [hep-ph].
- [26] T. Fukuyama, T. Kikuchi, and T. Osaka, *JCAP* **06**, 005 (2005), arXiv:hep-ph/0503201.
- [27] M. Endo, F. Takahashi, and T. T. Yanagida, *Phys. Rev. D* **74**, 123523 (2006), arXiv:hep-ph/0611055.
- [28] F. Hahn-Woernle and M. Plumacher, *Nucl. Phys. B* **806**, 68 (2009), arXiv:0801.3972 [hep-ph].
- [29] R. T. Co, Y. Mambrini, and K. A. Olive, *Phys. Rev. D* **106**, 075006 (2022), arXiv:2205.01689 [hep-ph].
- [30] B. Barman, S. Cléry, R. T. Co, Y. Mambrini, and K. A. Olive, (2022), arXiv:2210.05716 [hep-ph].
- [31] J. Martin, C. Ringeval, and V. Vennin, *Phys. Dark Univ.* **5-6**, 75 (2014), arXiv:1303.3787 [astro-ph.CO].
- [32] W. Buchmuller, P. Di Bari, and M. Plumacher, *Annals Phys.* **315**, 305 (2005), arXiv:hep-ph/0401240.
- [33] A. Pilaftsis and T. E. J. Underwood, *Nucl. Phys. B* **692**, 303 (2004), arXiv:hep-ph/0309342.
- [34] K. Moffat, S. Pascoli, S. T. Petcov, H. Schulz, and J. Turner, *Phys. Rev. D* **98**, 015036 (2018), arXiv:1804.05066 [hep-ph].
- [35] S. Dell’Oro, S. Marocco, M. Viel, and F. Vissani, *Adv. High Energy Phys.* **2016**, 2162659 (2016), arXiv:1601.07512 [hep-ph].
- [36] T. Endoh, S. Kaneko, S. K. Kang, T. Morozumi, and M. Tanimoto, *Phys. Rev. Lett.* **89**, 231601 (2002), arXiv:hep-ph/0209020.
- [37] I. Esteban, M. C. Gonzalez-Garcia, M. Maltoni, I. Martinez-Soler, and T. Schwetz, *JHEP* **01**, 087 (2017), arXiv:1611.01514 [hep-ph].

- [38] E. Bertuzzo, P. Di Bari, and L. Marzola, *Nucl. Phys. B* **849**, 521 (2011), [arXiv:1007.1641 \[hep-ph\]](#).
- [39] S. Ipek, A. D. Plascencia, and J. Turner, *JHEP* **12**, 111 (2018), [arXiv:1806.00460 \[hep-ph\]](#).
- [40] D. Croon, N. Fernandez, D. McKeen, and G. White, *JHEP* **06**, 098 (2019), [arXiv:1903.08658 \[hep-ph\]](#).
- [41] J. A. Dror, T. Hiramatsu, K. Kohri, H. Murayama, and G. White, *Phys. Rev. Lett.* **124**, 041804 (2020), [arXiv:1908.03227 \[hep-ph\]](#).
- [42] B. Barman, D. Borah, A. Dasgupta, and A. Ghoshal, *Phys. Rev. D* **106**, 015007 (2022), [arXiv:2205.03422 \[hep-ph\]](#).
- [43] A. Dasgupta, P. S. B. Dev, A. Ghoshal, and A. Mazumdar, (2022), [arXiv:2206.07032 \[hep-ph\]](#).
- [44] D. Borah, A. Dasgupta, and I. Saha, (2022), [arXiv:2207.14226 \[hep-ph\]](#).
- [45] D. I. Dunskey, A. Ghoshal, H. Murayama, Y. Sakakihara, and G. White, (2021), [arXiv:2111.08750 \[hep-ph\]](#).
- [46] N. Bhaumik, A. Ghoshal, and M. Lewicki, *JHEP* **07**, 130 (2022), [arXiv:2205.06260 \[astro-ph.CO\]](#).
- [47] M. Drewes, *JCAP* **03**, 013 (2016), [arXiv:1511.03280 \[astro-ph.CO\]](#).
- [48] M. Drewes, J. U. Kang, and U. R. Mun, *JHEP* **11**, 072 (2017), [arXiv:1708.01197 \[astro-ph.CO\]](#).
- [49] M. Drewes, *JCAP* **09**, 069 (2022), [arXiv:1903.09599 \[astro-ph.CO\]](#).
- [50] M. Drewes and L. Ming, (2022), [arXiv:2208.07609 \[hep-ph\]](#).
- [51] D. Maity and P. Saha, *Phys. Rev. D* **98**, 103525 (2018), [arXiv:1801.03059 \[hep-ph\]](#).
- [52] D. Maity and P. Saha, *Phys. Dark Univ.* **25**, 100317 (2019), [arXiv:1804.10115 \[hep-ph\]](#).
- [53] M. R. Haque, D. Maity, and P. Saha, *Phys. Rev. D* **102**, 083534 (2020), [arXiv:2009.02794 \[hep-th\]](#).
- [54] L. Kofman, A. D. Linde, and A. A. Starobinsky, *Phys. Rev. Lett.* **73**, 3195 (1994), [arXiv:hep-th/9405187](#).
- [55] L. Kofman, A. D. Linde, and A. A. Starobinsky, *Phys. Rev. D* **56**, 3258 (1997), [arXiv:hep-ph/9704452](#).
- [56] R. Kallosh and A. Linde, *JCAP* **06**, 028 (2013), [arXiv:1306.3214 \[hep-th\]](#).
- [57] R. Kallosh and A. Linde, *JCAP* **07**, 002 (2013), [arXiv:1306.5220 \[hep-th\]](#).
- [58] R. Kallosh, A. Linde, and D. Roest, *JHEP* **11**, 198 (2013), [arXiv:1311.0472 \[hep-th\]](#).
- [59] R. Kallosh and A. Linde, *JCAP* **06**, 027 (2013), [arXiv:1306.3211 \[hep-th\]](#).
- [60] R. Kallosh and A. Linde, *JCAP* **10**, 033 (2013), [arXiv:1307.7938 \[hep-th\]](#).
- [61] M. Galante, R. Kallosh, A. Linde, and D. Roest, *Phys. Rev. Lett.* **114**, 141302 (2015), [arXiv:1412.3797 \[hep-th\]](#).
- [62] P. A. R. Ade et al. (BICEP, Keck), *Phys. Rev. Lett.* **127**, 151301 (2021), [arXiv:2110.00483 \[astro-ph.CO\]](#).
- [63] F. L. Bezrukov and M. Shaposhnikov, *Phys. Lett. B* **659**, 703 (2008), [arXiv:0710.3755 \[hep-th\]](#).
- [64] N. Aghanim et al. (Planck), *Astron. Astrophys.* **641**, A6 (2020), [Erratum: *Astron. Astrophys.* 652, C4 (2021)], [arXiv:1807.06209 \[astro-ph.CO\]](#).
- [65] P. A. Zyla et al. (Particle Data Group), *PTEP* **2020**, 083C01 (2020).
- [66] S. Antusch, J. P. Baumann, V. F. Domcke, and P. M. Kostka, *JCAP* **10**, 006 (2010), [arXiv:1007.0708 \[hep-ph\]](#).
- [67] S. Antusch and K. Marschall, *JCAP* **05**, 015 (2018), [arXiv:1802.05647 \[hep-ph\]](#).
- [68] M. A. G. Garcia, K. Kaneta, Y. Mambrini, and K. A. Olive, *Phys. Rev. D* **101**, 123507 (2020), [arXiv:2004.08404 \[hep-ph\]](#).
- [69] G. F. Giudice, E. W. Kolb, and A. Riotto, *Phys. Rev. D* **64**, 023508 (2001), [arXiv:hep-ph/0005123](#).
- [70] Y. Hamada and K. Kawana, *Phys. Lett. B* **763**, 388 (2016), [arXiv:1510.05186 \[hep-ph\]](#).
- [71] Y. Hamada, K. Tsumura, and D. Yasuhara, *Phys. Rev. D* **95**, 103505 (2017), [arXiv:1608.05256 \[hep-ph\]](#).
- [72] K. D. Lozanov and M. A. Amin, *Phys. Rev. Lett.* **119**, 061301 (2017), [arXiv:1608.01213 \[astro-ph.CO\]](#).
- [73] J. A. Casas and A. Ibarra, *Nucl. Phys. B* **618**, 171 (2001), [arXiv:hep-ph/0103065](#).
- [74] K. Abazajian et al. (CMB-S4), *Astrophys. J.* **926**, 54 (2022), [arXiv:2008.12619 \[astro-ph.CO\]](#).
- [75] M. Hazumi et al., *J. Low Temp. Phys.* **194**, 443 (2019).
- [76] D. Adak, A. Sen, S. Basak, J. Delabrouille, T. Ghosh, A. Rotti, G. Martínez-Solaesche, and T. Souradeep, *Mon. Not. Roy. Astron. Soc.* **514**, 3002 (2022), [arXiv:2110.12362 \[astro-ph.CO\]](#).
- [77] J. T. Sayre et al. (SPT), *Phys. Rev. D* **101**, 122003 (2020), [arXiv:1910.05748 \[astro-ph.CO\]](#).
- [78] A. Suzuki et al. (POLARBEAR), *J. Low Temp. Phys.* **184**, 805 (2016), [arXiv:1512.07299 \[astro-ph.IM\]](#).
- [79] S. Aiola et al. (ACT), *JCAP* **12**, 047 (2020), [arXiv:2007.07288 \[astro-ph.CO\]](#).
- [80] K. Harrington et al., *Proc. SPIE Int. Soc. Opt. Eng.* **9914**, 99141K (2016), [arXiv:1608.08234 \[astro-ph.IM\]](#).
- [81] G. Addamo et al. (LSPE), *JCAP* **08**, 008 (2021), [arXiv:2008.11049 \[astro-ph.IM\]](#).
- [82] A. Mennella et al., *Universe* **5**, 42 (2019).
- [83] P. Ade et al. (Simons Observatory), *JCAP* **02**, 056 (2019), [arXiv:1808.07445 \[astro-ph.CO\]](#).
- [84] P. A. R. Ade et al. (SPIDER), *Astrophys. J.* **927**, 174 (2022), [arXiv:2103.13334 \[astro-ph.CO\]](#).
- [85] N. Sehgal et al., (2019), [arXiv:1906.10134 \[astro-ph.CO\]](#).
- [86] S. Aiola et al. (CMB-HD), (2022), [arXiv:2203.05728 \[astro-ph.CO\]](#).
- [87] S. Antusch, P. Di Bari, D. A. Jones, and S. F. King, *Phys. Rev. D* **86**, 023516 (2012), [arXiv:1107.6002 \[hep-ph\]](#).